Published in final edited form as:
J Neurochem. 2012 January ; 120(2): 292–301. doi:10.1111/j.1471-4159.2011.07572.x.

Inhibition of NADPH oxidase promotes alternative and anti–inflammatory microglial activation during neuroinflammation

Sang-Ho Choi[*,†], **Saba Aid**[*,†], **Hyung-Wook Kim**[†], **Sharon H. Jackson**[‡], and **Francesca Bosetti**[*,†,1]

[*]Molecular Neuroscience Unit, National Institutes of Health, Bethesda, Maryland, USA

[†]Brain Physiology and Metabolism Section, National Institute on Aging, National Institutes of Health, Bethesda, Maryland, USA

[‡]Monocyte Trafficking Unit, Laboratory of Host Defenses, National Institute of Allergy and Infectious Diseases, National Institutes of Health, Bethesda, Maryland, USA

Abstract

Like macrophages, microglia are functionally polarized into different phenotypic activation states, referred as classical and alternative. The balance of the two phenotypes may be critical to ensure proper brain homeostasis, and may be altered in brain pathological states, such as Alzheimer's disease. We investigated the role of NADPH oxidase in microglial activation state using $p47^{phox}$ and $gp91^{phox}$-deficient mice as well as apocynin, a NADPH oxidase inhibitor during neuroinflammation induced by an intracerebroventricular injection of LPS or $A\beta_{1–42}$. We showed that NADPH oxidase plays a critical role in the modulation of microglial phenotype and subsequent inflammatory response. We demonstrated that inhibition of NADPH oxidase or gene deletion of its functional $p47^{phox}$ subunit switched microglial activation from a classical to an alternative state in response to an inflammatory challenge. Moreover, we showed a shift in redox state towards an oxidized milieu and that subpopulations of microglia retain their detrimental phenotype in Alzheimer's disease brains. Microglia can change their activation phenotype depending on NADPH oxidase-dependent redox state of microenvironment. Inhibition of NADPH oxidase represents a promising neuroprotective approach to reduce oxidative stress and modulate microglial phenotype towards an alternative state.

Keywords

alternative activation; Alzheimer's disease; microglia; NADPH oxidase; neuroinflammation

NADPH oxidase is a multi-subunit enzyme complex responsible for the production of both extracellular and intracellular reactive oxygen species (ROS) by phagocytic cells including

Address correspondence and reprint request to Dr Bosetti, Molecular Neuroscience Unit, Brain Physiology and Metabolism Section, National Institute on Aging, National Institutes of Health, Bethesda, MD 20892-0947, USA. frances@mail.nih.gov and Dr Jackson, Laboratory of Host Defenses, NIAID, NIH, CRC Bldg 5-West Labs, Room 5-3942, 10 Center Drive, MSC 1456, Bethesda, MD 20892-1456. sjackson@niaid.nih.gov.
[1]Present address: National Institute of Neurological Disorders and Stroke, National Institutes of Health, 6001 Executive Blvd. Rm. 2118, Bethesda, MD 20892-9521, USA.

Supporting information
Additional supporting information may be found in the online version of this article:
Table S1. Demographic and quality characteristics of human subjects
As a service to our authors and readers, this journal provides supporting information supplied by the authors. Such materials are peer-reviewed and may be re-organized for online delivery, but are not copy-edited or typeset. Technical support issues arising from supporting information (other than missing files) should be addressed to the authors.

microglia. NADPH oxidase is comprised of cytoplasmic subunits ($p47^{phox}$, $p67^{phox}$, $p40^{phox}$, and Rac2), which upon phosphorylation by specific kinases can form a complex and translocate to the membrane to dock with the membrane subunits ($gp91^{phox}$ and $p22^{phox}$) (Babior 1999). NADPH oxidase expression is up-regulated in Alzheimer's disease (AD) (Shimohama *et al.* 2000; Bruce-Keller *et al.* 2010) and is an essential component of microglia-mediated amyloid neurotoxicity (Qin *et al.* 2002, 2004). Microglia are ubiquitously distributed throughout the brain and function as resident macrophages. They are highly dynamic and constantly carry out homeostatic surveillance to sense and respond to CNS abnormalities (Nimmerjahn *et al.* 2005). Upon detection of alterations in brain homeostasis, microglia undergo morphological and functional changes, referred to as microglial activation. Microglia are found surrounding amyloid plaques in the brain of AD patients and in transgenic AD mouse models (McGeer *et al.* 1987; Wyss-Coray 2006). However, whether activated microglia play detrimental or beneficial roles in AD remains to be elucidated.

In the last few years, much attention has been focused on the functional states of microglia rather than generalized activation by determining generic markers. Like peripheral macrophages, microglia are functionally polarized into different activation phenotypes during neuroinflammation. In the classical activation state, pro-inflammatory cytokines and ROS induce tissue damage and pathogen destruction, whereas the anti-inflammatory cytokine IL-4 induces an alternative activation state, characterized by the expression of arginase 1 (Arg1), Found in Inflammatory Zone 1 (Fizz1), mannose receptor 1 (Mrc1), and chitinase 3-like 3 (Chi3l3/Ym1), which dampen the inflammatory response and promote tissue repair and healing response (Martinez *et al.* 2008; Colton 2009). Recently, an age-dependent switch in the microglial phenotype from an alternative to a classical activation state has been reported in a transgenic mouse model of AD (Jimenez *et al.* 2008). Similarly, young and aged mice challenged with 1-methyl-4-phenyl-1,2,3,6-tetrahydropyridine exhibit age-related microglia activation and neurodegeneration (Sugama *et al.* 2003). At present, it is not clear why microglial activation significantly differs between young and aged mice, and how it is regulated in the aged brain or during the progression of neurodegenerative diseases. Thus, a better understanding of the mechanisms and functional significance of microglial activation state may provide novel therapeutic anti-inflammatory approaches. In this study, we show that gene deletion or pharmacological inhibition of NADPH oxidase drives microglial phenotype from a classical to an alternative activation state. Finally, we link NADPH oxidase-dependent effects on microglial activation state to the imbalance between markers of classical versus alternative microglial phenotype in the brain of AD patients.

Materials and methods

Animals and treatments

Male wild-type (WT), $p47^{phox-/-}$, and $gp91^{phox-/-}$ mice aged 10–12 weeks were used (Jackson *et al.* 1995). All procedures were approved by the National Institutes of Health (NIH) Animal Care and Use Committee in accordance with NIH guidelines on the care and use of laboratory animals. Intracerebroventricular (i.c.v.) injection was performed as previously described (Choi *et al.* 2008; Choi and Bosetti 2009). Under anesthesia (100 mg/kg ketamine plus 10 mg/kg xylazine, i.p.) and aseptic conditions, they received a single i.c.v injection of lipopolysaccharide (LPS) (5 μg; Sigma-Aldrich, St Louis, MO, USA), $A\beta_{1-42}$ (400 pmol; American Peptide, Sunnyvale, CA, USA), anti-IL-4 (4 ng; R&D Systems, Minneapolis, MN, USA) or vehicle (sterile saline) by using a syringe with a fine needle (World Precision Instruments, Sarasota, FL, USA) and a syringe pump (Stoelting, Wood Dale, IL, USA). The dose and time point (24 h) have been shown earlier to induce a robust neuroinflammatory response (Choi *et al.* 2008; Choi and Bosetti 2009). For pharmacological

inhibition of NADPH oxidase, apocynin (5 mg/kg; Sigma-Aldrich) was administered in WT mice by i.p. injection 30 min before LPS injection (Jackman *et al.* 2009). Injection coordinates were −2.3 mm dorsal/ventral, −1.0 mm lateral, and −0.5 mm anterior/posterior from the bregma and infusion rate was 0.5 μL/min. The needle was kept in this position for an additional 5 min after injection and then retrieved slowly out of the brain. After a survival time of 24 h, mice were killed and randomly included in either the biochemical or the histological study. The correct placement of the injection was verified during the histological process.

Histology

After transcardial perfusion with phosphate-buffered saline and subsequent 4% paraformaldehyde followed by cryoprotection in 30% sucrose at 4°C, cryostat section (30 μm) were cut coronally, collected free-floating, and stored in storage solution until processed (Choi *et al.* 2008). Sections were incubated in primary antibodies, rat anti-CD11b (Serotec, Raleigh, NC, USA), rat anti-7/4 (Serotec), rabbit anti-Ym1 (Stemcell Technologies, Vancouver, Canada), rabbit Macrophage Receptor with Collagenous structure (MARCO) (Santa Cruz Biotechnology, Santa Cruz, CA, USA) or rabbit anti-Iba-1 (Wako, Osaka, Japan) overnight followed by appropriate biotinylated secondary antibody (Vector Laboratories, Burlingame, CA, USA). For immunofluorescence staining, sections were incubated overnight in blocking buffer containing primary antibodies and then secondary antibodies conjugated to Alexa Fluor dye (Invitrogen, Carlsbad, CA, USA). Images were collected on a LSM 510 confocal microscope (Zeiss, Thornwood, NY, USA).

Quantitative real-time PCR analysis

Total RNA was isolated with RNeasy Lipid Tissue Midi Kit (Qiagen, Valencia, CA, USA) and reverse transcription was performed with cDNA reverse transcription kit (Applied Biosystems, Carlsbad, CA, USA) according to the manufacturer's instructions (Choi *et al.* 2008). Quantitative real-time PCR was performed using a 7000 Real-time PCR System (Applied Biosystems). Relative mRNA levels were calculated according to the $2^{-\Delta\Delta Ct}$ method. All ΔCT values were normalized to phosphoglycerate kinase 1 or glyceraldehydes-3-phosphate dehydrogenase.

Immunoblot analysis

Brain samples were homogenized in RIPA buffer (Cell Signaling Technology, Danvers, MA, USA). Samples were then denatured, and equivalent amounts of protein were separated by standard sodium dodecyl sulfate–polyacrylamide gel electrophoresis (Bio-Rad Laboratories, Hercules, CA, USA) and blotted onto polyvinylidene difluoride. Primary antibodies to the following proteins were used: $p47^{phox}$ (BD Biosciences, San Jose, CA, USA), Y (Stemcell Technologies) and β-actin (Sigma-Aldrich). After incubation with primary antibodies, blots were washed and exposed to fluorochrome-conjugated secondary antibodies and scanned by using an Odyssey Infrared Imaging System (Li-Cor Biosciences, Lincoln, Nebraska).

ELISA

IL-4 (eBioscience, San Diego, CA, USA) and myeloperoxidase (Cell Sciences, Canton, MA, USA) were assessed by ELISA following the manufacturer's instructions.

Postmortem human brain tissues

Frozen postmortem human frontal cortex (Brodmann area 9) was provided by the Harvard Brain Tissue Resource Center (McLean Hospital, Belmont, MA, USA). The study was approved by the Institutional Review Boards of the McLean Hospital and of the National

Institute on Aging, NIH, and by the Office of Human Subjects Research of NIH protocol (#4380). The study was performed on tissue from 10 AD patients (stage V or VI of AD) (Reisberg *et al.* 2008) and 10 age-matched controls (Table S1). Brain pH was measured as previously described (Harrison *et al.* 1995). Mean ± SEM values of age (years) (control 70.20 ± 2.4 vs. AD 70.60 ± 2.4), postmortem interval (h) (control 19.16 ± 1.0 vs. AD 19.74 ± 1.0), and brain pH (control 6.76 ± 0.07 vs. AD 6.84 ± 0.07) did not differ significantly between the two groups. AD patients were under various antidepressant and antipsychotic medications.

Statistical analysis

Data are presented as means ± SEM. Differences in mean values were compared by *t*-test or ANOVA and were considered significant at $p < 0.05$.

Results

Deletion of p47^{phox} subunit modulates microglial activation status and reduces leukocyte infiltration

To elucidate whether the deletion of p47^{phox} subunit would affect classical microglial activation and the associated inflammatory response, we examined its morphological changes, the expression of cell surface molecules, and inflammatory factors. In vehicle-injected controls, CD11b^{+} cells possessed thin processes that branched several times as they extended from the small cell bodies (Fig. 1a and c), whereas CD11b^{+} cells in the hippocampus of WT mice appeared activated 24 h after i.c.v. injection of LPS. Their cell bodies were hypertrophic had fewer processes, and those processes were thicker and shorter (Fig. 1b). In some cases, CD11b^{+} cells were amoeboid with few or no processes (Fig. 1b). In contrast, CD11b^{+} cells showed a different morphology in LPS-injected p47$^{phox-/-}$ mice. Their cell bodies were hypertrophic, and had thick and ramified processes (Fig. 1d). In addition, the intensity of Iba-1 immunoreactivity and number of Iba-1^{+} cells were lower 24 h after i.c.v. injection of LPS in p47$^{phox-/-}$ mice compared with WT mice (Fig. 1h and i). Furthermore, mRNA expression of Iba-1 was significantly reduced in p47$^{phox-/-}$ mice (Fig. 1j), along with the significant reduction of pro-inflammatory factors such as TNF-α, chemokine (C-C motif) ligand 2 (CCL2), and chemokine (C-C motif) receptor 2 (CCR2) (Fig. 1k–m). IL-1β mRNA expression was not significantly changed (Fig. 1n). Consistent with the mRNA findings, no significant decrease in protein levels of IL-1β was found in p47$^{phox-/-}$ after LPS (data not shown).

Peripheral leukocytes infiltrate the CNS after various inflammatory stimuli and can exacerbate brain tissue injury by releasing various cytotoxic and inflammatory mediators and increasing vascular permeability (Shaftel *et al.* 2008; Choi *et al.* 2010). To investigate whether the presence or absence of NADPH oxidase could modify leukocyte recruitment, we examined their infiltration by immunohistochemistry using the 7/4 antibody as a specific marker of neutrophils at 24 h after i.c.v. injection of LPS. After LPS injection, the number of 7/4^{+} cells was significantly reduced in the hippocampus of mice lacking p47^{phox} (Fig. 2d and e) compared with their WT controls (Fig. 2b and e). Vehicle-injected mice showed no genotype-related differences (Fig. 2a and c). Supporting these data, levels of brain myeloperoxidase were significantly reduced in mice lacking p47^{phox} compared with WT mice (Fig. 2f).

Deletion of p47^{phox} subunit promotes alternative microglial activation

To further investigate whether the deletion of p47^{phox} subunit could modify microglial activation, we examined its phenotype and the expression of anti-inflammatory factors. Brain levels of IL-4 and expression of IL-4 receptor alpha (IL-4Rα) mRNA were

significantly increased 24 h after i.c.v. injection of LPS in $p47^{phox-/-}$ mice compared with WT mice (Fig. 3a and b). This up-regulation of IL-4 was concomitant with a marked induction in the expression of genes encoding Ym1 and Fizz1 and Ym1 protein in $p47^{phox-/-}$ mice compared with WT mice (Fig. 3c and d). In vehicle-injected mice, an induction of Ym1 and Fizz1 was barely detectable (data not shown). Similarly, mRNA expression for the two scavenger receptors CD163 and MARCO, which have also been shown to be expressed in anti-inflammatory activated microglia/macrophages (Kraal *et al.* 2000; McGeer and McGeer 2008), was significantly increased 24 h after i.c.v. injection of LPS in $p47^{phox-/-}$ mice (Fig. 3c).

By using immunostaining and quantitative PCR, we further determined the cellular origin of alternative activation markers. At 24 h after LPS injection, the intensity of Ym1 and MARCO immunoreactivity was increased in the hippocampus of mice lacking $p47^{phox}$ (Fig. 3h and l) compared with their WT controls (Fig. 3f and j). Vehicle-injected mice showed no genotype-related differences. We also performed quantitative PCR to analyze Ym1 expression in microglia freshly isolated from mice at 24 h after the LPS challenge. Microglia from $p47^{phox-/-}$ mice had significantly higher Ym1 and MARCO expression compared with WT mice (Fig. 3m and n). To corroborate this result, we performed double-immunofluorescence staining with cell type-specific markers in $p47^{phox-/-}$ mice after LPS challenge. The $Ym1^+$ cells were identified as microglia by its colocalization with MARCO (Fig. 4a). Ym1 immunoreactivity was not detected in $GFAP^+$ astrocytes and $NeuN^+$ neurons (Fig. 4b and c). These results indicate that deletion of $p47^{phox}$ subunit alters the cytokine profile of the brain and elevates the subpopulation of alternatively activated microglia.

Deletion of $gp91^{phox}$ subunit or inhibition of NADPH oxidase enhances alternative microglial activation and attenuates the pro-inflammatory response

To ascertain whether the alteration of activation phenotype and inflammatory response observed in $p47^{phox-/-}$ mice was attributable to change in NADPH oxidase-derived O_2^- generation, we confirmed our findings using WT mice pre-treated with apocynin, a selective inhibitor for NADPH oxidase (Wang *et al.* 2006; Jackman *et al.* 2009) or mice lacking $gp91^{phox}$ subunit. Consistent with the data obtained in $p47^{phox-/-}$ mice, pre-treatment of WT mice with apocynin enhanced the mRNA expression of Ym1 and MARCO (Fig. 5a and b), and decreased the mRNA expression of pro-inflammatory factors TNF-α and CCL2 at 24 h after i.c.v. injection of LPS (Fig. 5c and d). Similarly, expression of Ym1 and MARCO mRNA was significantly increased in $gp91^{phox-/-}$ mice compared with their respective WT mice after i.c.v. LPS injection (Fig. 5e and f). In addition, expression of IL-4Rα mRNA was significantly increased in $gp91^{phox-/-}$ mice compared with their respective WT mice (data not shown). Although a trend towards a decrease in mRNA expression was observed for TNF-α and CCR2 in $gp91^{phox-/-}$ mice, it did not reach statistical significance (Fig. 5g and h). These consistent findings in two different genetic models and after inhibition of NADPH oxidase with apocynin support the critical role of NADPH oxidase in regulating microglial phenotype and inflammatory response.

$p47^{phox-/-}$ mice acquire alternatively activated phenotype of microglia after $A\beta_{1-42}$ challenge

To further investigate whether ligation of pathogen recognition receptors would lead to worsen neuroinflammation and change microglial phenotypes in WT mice compared with $p47^{phox-/-}$ mice, similar to what we observed with LPS challenge. We injected $A\beta_{1-42}$ into the lateral ventricle of WT and $p47^{phox-/-}$ mice to induce inflammation. Consistent with the LPS data, expression of Ym1 mRNA was significantly increased in $p47^{phox-/-}$ mice (Fig. 6a), whereas expression of CCL2 mRNA was markedly decreased in $p47^{phox-/-}$ mice compared with WT mice at 24 h after i.c.v. injection of $A\beta_{1-42}$ (Fig. 6b).

Neutralization of IL-4 markedly suppresses alternative microglia activation and enhances the pro-inflammatory response

To further elucidate whether anti-inflammatory cytokine IL-4 and its receptor IL-4α is specifically causing the induction of alternative activation in $p47^{phox-/-}$ mice, we examined its effect by neutralization using a specific IL-4 neutralizing antibody. At 24 h after coinjection with LPS, the expression of genes encoding for Ym1 and Fizz1 was considerably lower in $p47^{phox-/-}$ mice compared with IgG-treated $p47^{phox-/-}$ mice (Fig. 7a). In contrast, the expression of genes encoding for TNF-α and CCL2 was significantly increased in $p47^{phox-/-}$ mice (Fig. 7b). In addition, neutralization of IL-4 also enhanced the CD40 and Iba-1 mRNA expression compared with IgG-treated $p47^{phox-/-}$ mice (Fig. 7c). These results indicate that among various bioactive factors released from activated microglia, IL-4 might play crucial role in promoting signal transduction resulting in alternative activation.

NADPH oxidase $p47^{phox}$ subunit is up-regulated in the brains of AD patients

To determine whether $p47^{phox}$ expression was altered in AD patients, we assessed $p47^{phox}$ mRNA in the frontal cortex from postmortem AD brains. AD samples had increased $p47^{phox}$ mRNA compared with age-matched controls (Fig. 8). In the AD brain, the expression of $p47^{phox}$ mRNA increased approximately two-fold, whereas the expression of the antioxidant enzymes glutathione peroxidase 1 and superoxide dismutase 1 mRNA significantly decreased compared with age-matched controls (Fig. 8), indicating that there may be an inverse correlation between regional O_2^- production and its scavenging. Furthermore, AD samples showed a significant alteration of pro- and anti-inflammatory factors, such as Arg1, Arg2, Mrc1, and CD11b (Fig. 8). These results support an age-and disease- related shift in redox state towards an oxidized environment with subpopulations of microglia showing an imbalance towards a classical/detrimental phenotype versus an alternative phenotype in brains of AD patients.

Discussion

While NADPH oxidase has been implicated in AD and other neurodegenerative disorders, in this study, we report for the first time that NADPH oxidase during neuroinflammation plays a critical role in modulating the microglial phenotype towards a pro-inflammatory, classically activated state. We demonstrate that gene deletion or inhibition of NADPH oxidase modulates microglial phenotype in inflamed brain and in these conditions microglia acquire anti-inflammatory phenotype through IL-4-dependent signaling pathway. Up-regulation of brain NADPH oxidase expression during aging and in animal models and postmortem clinical samples of AD suggests a role for NADPH oxidase in the susceptibility of the aging brain to neurodegenerative diseases and in the progression of the pro-inflammatory response in AD. These findings suggest that NADPH oxidase acts as a guide and regulates the age-related increase in detrimental microglial activation and the accompanying increase in oxidative stress in AD.

Over the last two decades the question of whether activated microglia play harmful or helpful roles in acute CNS injuries and neurodegenerative diseases has been widely debated (Wyss-Coray 2006; Streit 2010). Neurode-generative diseases, including AD, are characterized by slowly progressive neurodegeneration that may take decades to develop. In this chronic neurodegenerative disease, activated microglia has been demonstrated to play both detrimental and beneficial roles (Lynch 2009; Neumann *et al.* 2009). One possible explanation for the persistent Aβ accumulation and AD progression despite increasing microglial activation is that with aging and disease microglia change their phenotype to a pro-inflammatory, classically activated, state and lose their phagocytic capabilities. In the

last decade, much attention has been paid to the functional states of microglia and several groups have focused on the roles for microglial activation phenotypes in the progression of AD. A previous study on transcription profiles for microglia shows the coexistence of pro-inflammatory classical activation state and the counterbalancing anti-inflammatory alternative activation states in the brain of AD patients and in mouse models of AD (Colton *et al.* 2006). However, a recent study demonstrates an age-dependent phenotypic change of microglial activation in the hippocampus of transgenic AD mice from an alternative activation state with Aβ phagocytic capabilities to a classical cytotoxic phenotype, which promotes high levels of soluble Aβ oligomers and significant pyramidal neurodegeneration (Jimenez *et al.* 2008). Although these results are conflicting, they show that microglia change their activation phenotypes during the progression of AD. Thus, an imbalance of two phenotypes toward an abnormal increase of the classical activation phenotype and reduction of the anti-inflammatory alternative activation and phagocytic capabilities might contribute significantly to the progression of AD pathology. Thus, it is important to identify the intrinsic factors that, in addition to aging, promote a shift of microglial phenotype, and how to pharmacologically modulate the age- or disease-dependent changes in microglial activation state.

The expression of NADPH oxidase, an essential component of microglia-mediated Aβ neurotoxicity (Qin *et al.* 2002), is up-regulated in postmortem brains from patients with AD and mild cognitive impairment (Shimohama *et al.* 2000; Bruce-Keller *et al.* 2010). Moreover, transgenic mouse models of AD lacking $gp91^{phox}$ do not show oxidative stress, cerebrovascular damage, and behavioral deficits (Park *et al.* 2008). These studies suggest that NADPH oxidase could contribute to the oxidative stress associated with AD, and also implicate its role in regulating signaling pathway. Previous studies using LPS and $A\beta_{1–42}$ to activate microglia show that only NADPH oxidase from microglia mediates neuronal damage (Qin *et al.* 2002, 2004). Furthermore, isolated microglia from $gp91^{phox-/-}$ mice failed to produce extracellular superoxide, expressed lower pro-inflammatory cytokines, and showed significantly less intracellular ROS (Qin *et al.* 2004). Thus, microglia are the predominant source of NADPH oxidase-derived ROS and targeting microglial NADPH oxidase can be an ideal approach to attenuate detrimental activation of microglia in AD (Wilkinson and Landreth 2006; Block 2008). We show here that the expression of $p47^{phox}$, the regulatory subunit of NADPH oxidase, is increased in the brains from AD patients and is specifically localized in activated microglia. Conversely, the expression of the antioxidant enzymes glutathione peroxidase 1 and superoxide dismutase 1 is significantly decreased in AD patients compared with age-matched controls, indicating that an inverse correlation between regional O_2^- formation and its scavenging. According to the oxidative stress theory of aging, with age there is a disruption in the delicate balance between ROS generation and antioxidant/buffering systems, which leads to a shift to an oxidative cellular milieu. Experimental elevations in the endogenous antioxidant glutathione and in dietary antioxidants in the AD brain are capable of reducing oxidative damage and delaying the progression of the disease (Aliev *et al.* 2008). Furthermore, previous *in vitro* studies using cultured microglia have shown that redox state modulates microglial proliferation and function, which were attributed to ROS generated by the NADPH oxidase (Pawate *et al.* 2004; Mander *et al.* 2006). Thus, we hypothesize that conditions that increase NADPH oxidase activity and the gradual decline in antioxidant capacity during aging, may contribute to acquire and retain microglia in the pro-inflammatory classical activation state. In this study, we indicate that NADPH oxidase is a plausible candidate to modulate microglia activation in AD. We show that the gene deletion or pharmacological inhibition of NADPH oxidase drives microglial phenotype from classical to alternative activation. These results suggest that age-related, NADPH oxidase-dependent shift in the redox state towards an oxidized environment results in subpopulations of microglia retaining their detrimental, pro-inflammatory phenotype in brains of AD patients. Thus, inhibition of NADPH oxidase

represents a potential therapeutic approach to reduce oxidative stress and to promote the switch of microglial activation towards an alternative, anti-inflammatory phenotype.

Supplementary Material

Refer to Web version on PubMed Central for supplementary material.

Acknowledgments

We acknowledge the Harvard Brain Tissue Resource Center (McLean Hospital, Belmont, MA) and Dr J.S. Rao (NIA, NIH) for providing human tissue samples, and Dr S.H. Park (NINDS, NIH) for assistance with confocal microscopy. This work was supported by the Intramural Research Program of the National Institute on Aging, National Institutes of Health.

Abbreviations used

AD	Alzheimer's disease
Arg	arginase
CCL2	chemokine (C-C motif) ligand 2
CCR2	chemokine (C-C motif) receptor 2
Fizz1	Found in Inflammatory Zone 1
LPS	lipopolysaccharide
MARCO	Macrophage Receptor with Collagenous structure
ROS	reactive oxygen species
WT	wild-type

References

Aliev G, Obrenovich ME, Reddy VP, Shenk JC, Moreira PI, Nunomura A, Zhu X, Smith MA, Perry G. Anti-oxidant therapy in Alzheimer's disease: theory and practice. Mini Rev Med Chem. 2008; 8:1395–1406. [PubMed: 18991755]

Babior BM. NADPH oxidase: an update. Blood. 1999; 93:1464–1476. [PubMed: 10029572]

Block ML. NADPH oxidase as a therapeutic target in Alzheimer's disease. BMC Neurosci. 2008; 9(Suppl 2):S8. [PubMed: 19090996]

Bruce-Keller AJ, Gupta S, Parrino TE, Knight AG, Ebenezer PJ, Weidner AM, LeVine H III, Keller JN, Markesbery WR. NOX activity is increased in mild cognitive impairment. Antioxid Redox Signal. 2010; 12:1371–1382. [PubMed: 19929442]

Choi SH, Bosetti F. Cyclooxygenase-1 null mice show reduced neuroinflammation in response to beta-amyloid. Aging (Albany NY). 2009; 1:234–244. [PubMed: 20157512]

Choi SH, Langenbach R, Bosetti F. Genetic deletion or pharmacological inhibition of cyclooxygenase-1 attenuate lipopolysaccharide-induced inflammatory response and brain injury. FASEB J. 2008; 22:1491–1501. [PubMed: 18162486]

Choi SH, Aid S, Choi U, Bosetti F. Cyclooxygenases-1 and -2 differentially modulate leukocyte recruitment into the inflamed brain. Pharmacogenomics J. 2010; 10:448–457. [PubMed: 20038958]

Colton CA. Heterogeneity of microglial activation in the innate immune response in the brain. J Neuroimmune Pharmacol. 2009; 4:399–418. [PubMed: 19655259]

Colton CA, Mott RT, Sharpe H, Xu Q, Van Nostrand WE, Vitek MP. Expression profiles for macrophage alternative activation genes in AD and in mouse models of AD. J Neuroinflammation. 2006; 3:27. [PubMed: 17005052]

Harrison PJ, Heath PR, Eastwood SL, Burnet PW, McDonald B, Pearson RC. The relative importance of premortem acidosis and postmortem interval for human brain gene expression studies: selective

mRNA vulnerability and comparison with their encoded proteins. Neurosci Lett. 1995; 200:151–154. [PubMed: 9064599]

Jackman KA, Miller AA, De Silva TM, Crack PJ, Drummond GR, Sobey CG. Reduction of cerebral infarct volume by apocynin requires pretreatment and is absent in Nox2-deficient mice. Br J Pharmacol. 2009; 156:680–688. [PubMed: 19175604]

Jackson SH, Gallin JI, Holland SM. The p47phox mouse knock-out model of chronic granulomatous disease. J Exp Med. 1995; 182:751–758. [PubMed: 7650482]

Jimenez S, Baglietto-Vargas D, Caballero C, et al. Inflammatory response in the hippocampus of PS1M146L/APP751SL mouse model of Alzheimer's disease: age-dependent switch in the microglial phenotype from alternative to classic. J Neurosci. 2008; 28:11650–11661. [PubMed: 18987201]

Kraal G, van der Laan LJ, Elomaa O, Tryggvason K. The macrophage receptor MARCO. Microbes Infect. 2000; 2:313–316. [PubMed: 10758408]

Lynch MA. The multifaceted profile of activated microglia. Mol Neurobiol. 2009; 40:139–156. [PubMed: 19629762]

Mander PK, Jekabsone A, Brown GC. Microglia proliferation is regulated by hydrogen peroxide from NADPH oxidase. J Immunol. 2006; 176:1046–1052. [PubMed: 16393992]

Martinez FO, Sica A, Mantovani A, Locati M. Macrophage activation and polarization. Front Biosci. 2008; 13:453–461. [PubMed: 17981560]

McGeer PL, McGeer EG. Glial reactions in Parkinson's disease. Mov Disord. 2008; 23:474–483. [PubMed: 18044695]

McGeer PL, Itagaki S, Tago H, McGeer EG. Reactive microglia in patients with senile dementia of the Alzheimer type are positive for the histocompatibility glycoprotein HLA-DR. Neurosci Lett. 1987; 79:195–200. [PubMed: 3670729]

Neumann H, Kotter MR, Franklin RJ. Debris clearance by microglia: an essential link between degeneration and regeneration. Brain. 2009; 132:288–295. [PubMed: 18567623]

Nimmerjahn A, Kirchhoff F, Helmchen F. Resting microglial cells are highly dynamic surveillants of brain parenchyma in vivo. Science. 2005; 308:1314–1318. [PubMed: 15831717]

Park L, Zhou P, Pitstick R, et al. Nox2-derived radicals contribute to neurovascular and behavioral dysfunction in mice overexpressing the amyloid precursor protein. Proc Natl Acad Sci U S A. 2008; 105:1347–1352. [PubMed: 18202172]

Pawate S, Shen Q, Fan F, Bhat NR. Redox regulation of glial inflammatory response to lipopolysaccharide and interferongamma. J Neurosci Res. 2004; 77:540–551. [PubMed: 15264224]

Qin L, Liu Y, Cooper C, Liu B, Wilson B, Hong JS. Microglia enhance beta-amyloid peptide-induced toxicity in cortical and mesencephalic neurons by producing reactive oxygen species. J Neurochem. 2002; 83:973–983. [PubMed: 12421370]

Qin L, Liu Y, Wang T, Wei SJ, Block ML, Wilson B, Liu B, Hong JS. NADPH oxidase mediates lipopolysaccharide-induced neurotoxicity and proinflammatory gene expression in activated microglia. J Biol Chem. 2004; 279:1415–1421. [PubMed: 14578353]

Reisberg B, Prichep L, Mosconi L, et al. The pre-mild cognitive impairment, subjective cognitive impairment stage of Alzheimer's disease. Alzheimers Dement. 2008; 4:S98–S108. [PubMed: 18632010]

Shaftel SS, Griffin WS, O'Banion MK. The role of interleukin-1 in neuroinflammation and Alzheimer disease: an evolving perspective. J Neuroinflammation. 2008; 5:7. [PubMed: 18302763]

Shimohama S, Tanino H, Kawakami N, et al. Activation of NADPH oxidase in Alzheimer's disease brains. Biochem Biophys Res Commun. 2000; 273:5–9. [PubMed: 10873554]

Streit WJ. Microglial activation and neuroinflammation in Alzheimer's disease: a critical examination of recent history. Front Aging Neurosci. 2010; 2:22. [PubMed: 20577641]

Sugama S, Yang L, Cho BP, DeGiorgio LA, Lorenzl S, Albers DS, Beal MF, Volpe BT, Joh TH. Age-related microglial activation in 1-methyl-4-phenyl-1, 2, 3, 6-tetrahydropyridine (MPTP)-induced dopaminergic neurodegeneration in C57BL/6 mice. Brain Res. 2003; 964:288–294. [PubMed: 12576189]

Wang Q, Tompkins KD, Simonyi A, Korthuis RJ, Sun AY, Sun GY. Apocynin protects against global cerebral ischemia-reperfusion-induced oxidative stress and injury in the gerbil hippocampus. Brain Res. 2006; 1090:182–189. [PubMed: 16650838]

Wilkinson BL, Landreth GE. The microglial NADPH oxidase complex as a source of oxidative stress in Alzheimer's disease. J Neuroinflammation. 2006; 3:30. [PubMed: 17094809]

Wyss-Coray T. Inflammation in Alzheimer disease: driving force, bystander or beneficial response? Nat Med. 2006; 12:1005–1015. [PubMed: 16960575]

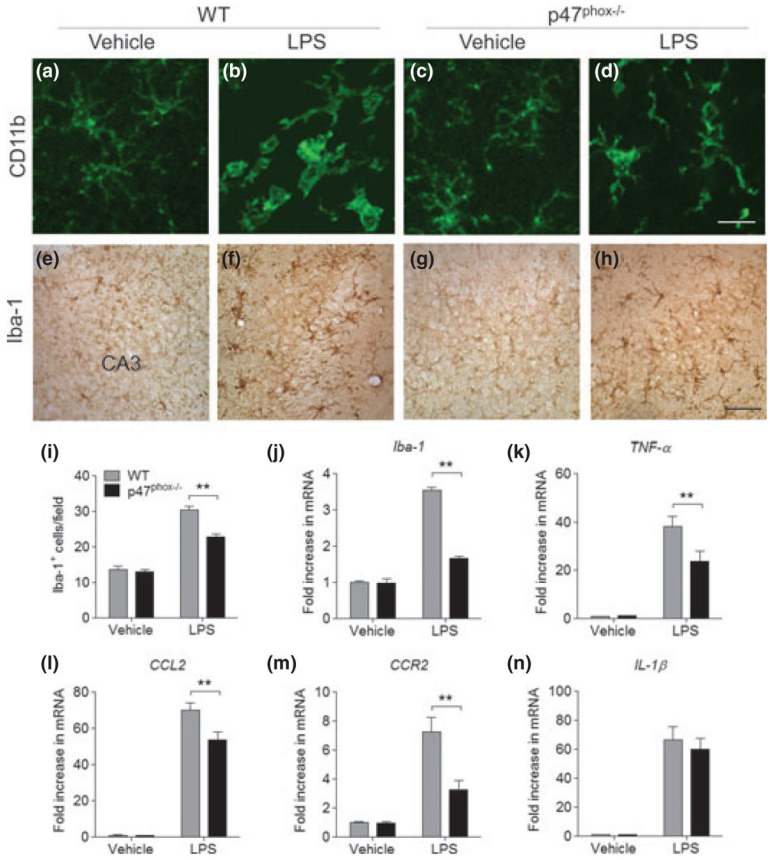

Fig. 1.

p47$^{phox-/-}$ mice show reduced microglia accumulation. (a–h) Immunostaining for microglia in the hippocampus of p47$^{phox-/-}$ and WT mice at 24 h after LPS, with antibodies to CD11b and Iba-1. Scale bar: (a–d) 50 μm; (e–h) 100 μm. (i) Quantitation of Iba-1^{+} cells showed a significant decrease of microglia accumulation in p47$^{phox-/-}$ mice compared with WT mice. Mean ± SEM ($n = 6$), $^{**}p < 0.01$. (j–n) Quantitative real-time PCR analysis showing expression of Iba-1, TNF-α, CCL2, CCR2, and IL-1β (relative to Pgk1) in p47$^{phox-/-}$ and WT mice. Mean ± SEM ($n = 6$), $^{**}p < 0.01$.

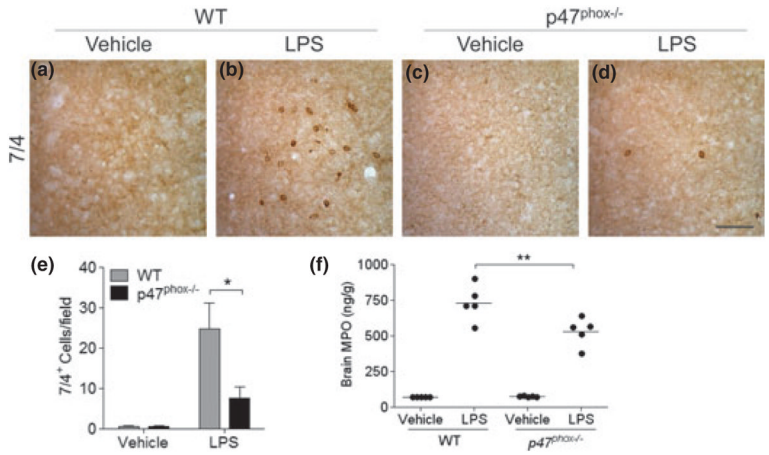

Fig. 2.

p47$^{phox-/-}$ mice show reduced peripheral leukocyte infiltration. (a–d) Immunostaining for neutrophils in the hippocampus of p47$^{phox-/-}$ and WT mice at 24 h after LPS, with 7/4 antibody. Scale bar, 100 μm. (e) Quantitation of 7/4^{+} cells showed a significant decrease of neutrophil infiltration in p47$^{phox-/-}$ mice compared with WT mice. Mean ± SEM ($n = 6$), *$p < 0.05$. (f) Brain MPO protein levels were measured in supernatants from WT and p47$^{phox-/-}$ mice at 24 h after LPS by ELISA. Mean ± SEM ($n = 5$), **$p < 0.01$.

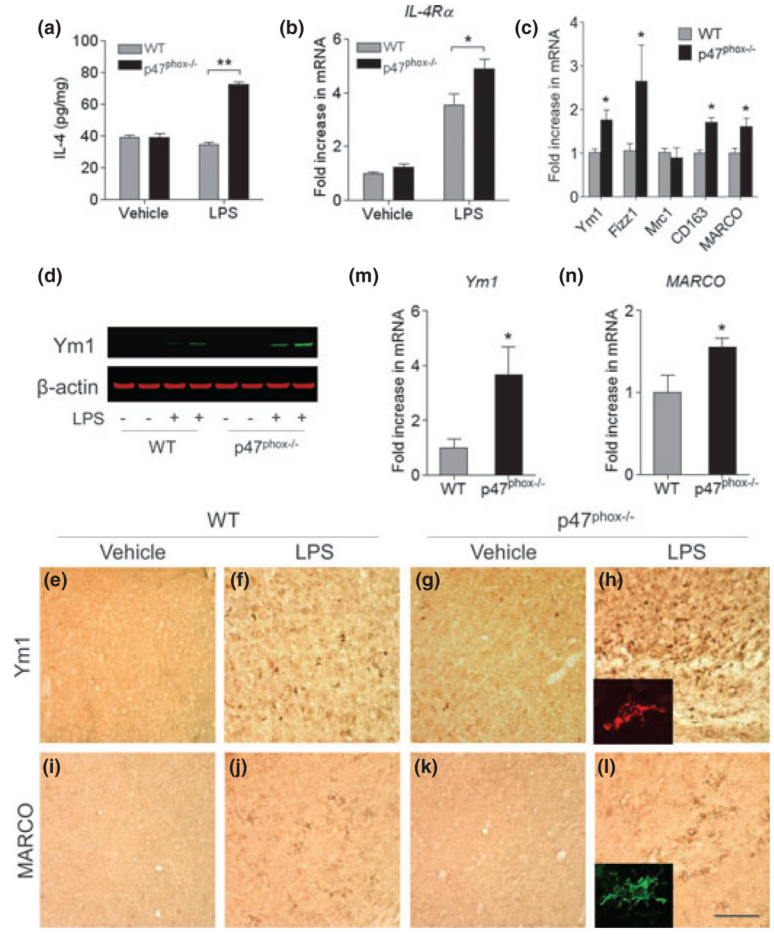

Fig. 3.

Gene deletion of p47^{phox} alters microglia phenotype. (a) ELISA showing production of brain IL-4 in p47$^{phox-/-}$ and WT mice. (b, c) Quantitative real-time PCR analysis showing expression of IL-4Rα, Ym1, Fizz1, Mrc1, CD163, and MARCO mRNA (relative to Pgk1) in p47$^{phox-/-}$ and WT mice. Mean ± SEM ($n = 6$), *$p < 0.05$, **$p < 0.01$. (d) Immunoblot showing protein levels of Ym1 in p47$^{phox-/-}$ and WT mice. (e–l) Immunostaining for the Ym1 and MARCO in the hippocampus of p47$^{phox-/-}$ and WT mice. Scale bar, 100 μm. Insets, immunofluorescence staining of Ym1^{+} and MARCO^{+} cells in p47$^{phox-/-}$ mice. (m, n) Induction of microglial Ym1 and MARCO. Brain microglia were isolated from WT and p47$^{phox-/-}$ mice at 24 h after LPS challenge and analyzed mRNA expression of Ym1 and MARCO by quantitative PCR. Mean ± SEM ($n = 3$), *$p < 0.05$. RNA, protein, and tissue samples were prepared from brains of WT and p47$^{phox-/-}$ mice at 24 h after LPS.

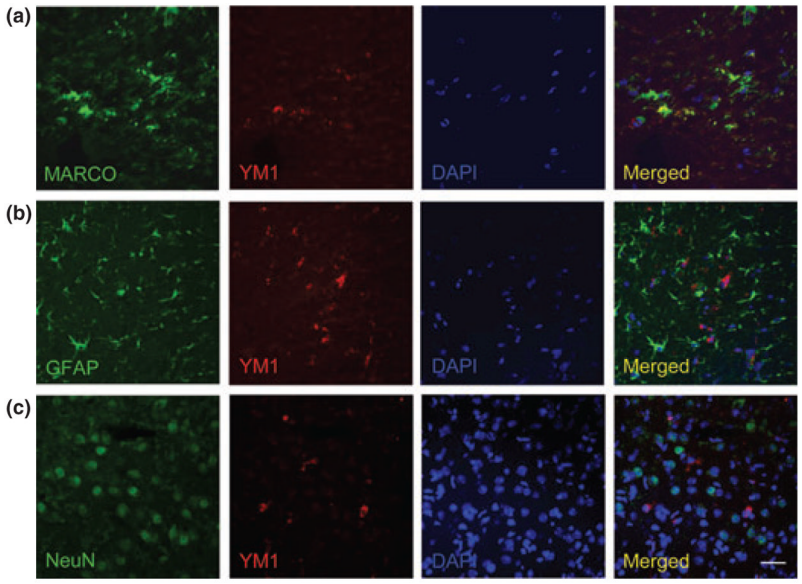

Fig. 4.

Ym1 is primarily expressed in alternatively activated microglia during inflammatory response. (a–c) Immunofluorescence staining with antibodies to MAR-CO, GFAP, NeuN, and Ym1 in the hippocampus of $p47^{phox-/-}$ mice, showing that the $Ym1^{+}$ cells overlaps precisely with $MARCO^{+}$ microglia. Tissue samples were prepared from brains of $p47^{phox-/-}$ mice at 24 h after LPS. Scale bar, 25 μm.

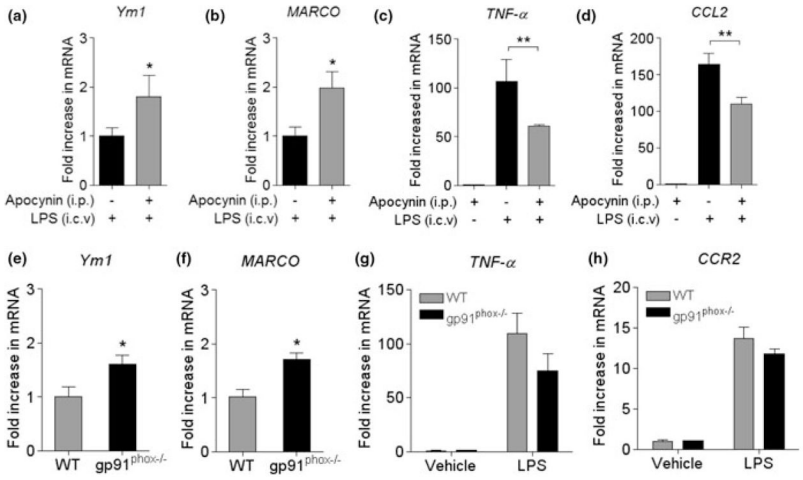

Fig. 5.

Inhibition of NADPH oxidase and gene deletion of gp91^{phox} modulates microglial activation phenotypes. (a–d) Quantitative real-time PCR analysis showing expression of Ym1, MARCO, TNF-α, and CCL2 mRNA (relative to Pgk1) in WT mice pre-treated with apocynin. (e–h) The Ym1, MARCO, TNF-α, and CCR2 mRNA expression (relative to Pgk1) in WT and gp91$^{phox-/-}$ mice was measured by quantitative PCR. RNA samples were prepared from brains of WT and p47$^{phox-/-}$ mice at 24 h after LPS. Mean ± SEM ($n = 5$), *$p < 0.05$, **$p < 0.01$.

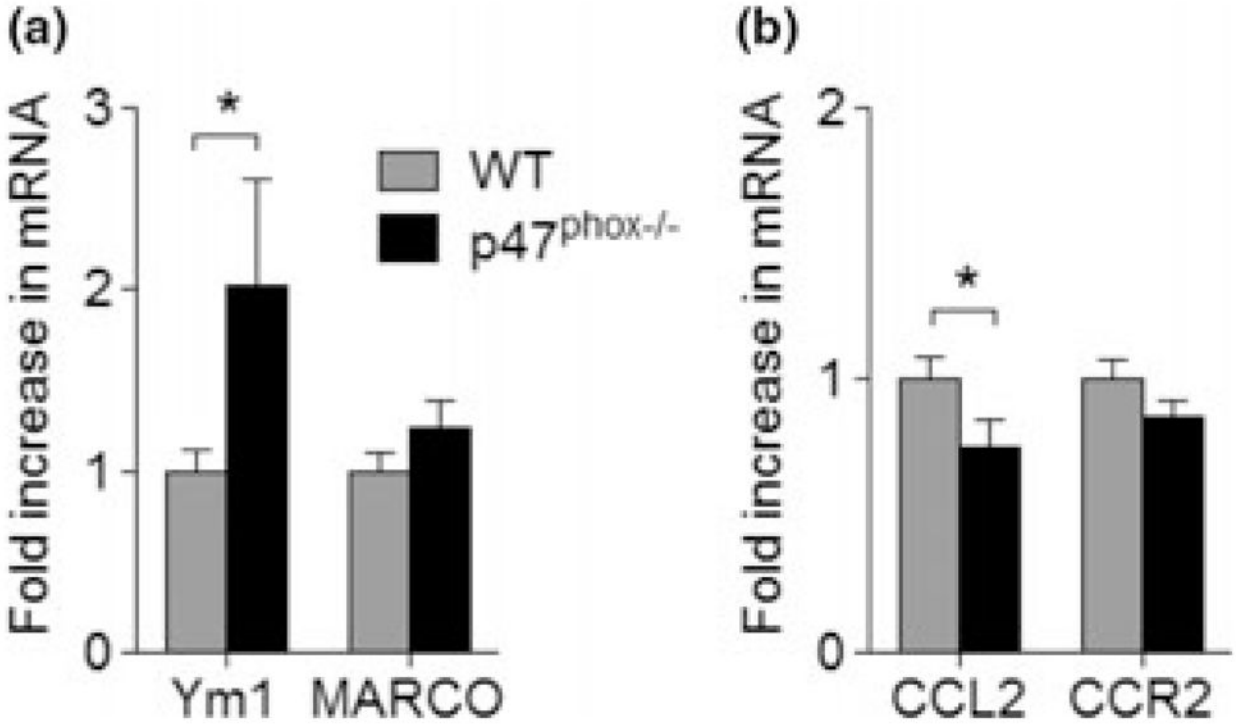

Fig. 6.

Effects of p47^{phox} deficiency on A$\beta_{1–42}$-induced microglial activation. (a, b) Quantitative real-time PCR analysis showing expression of Ym1, MARCO, CCL2, and CCR2 mRNA (relative to Pgk1) in p47$^{phox-/-}$ and WT mice. RNA samples were prepared from brains of WT and p47$^{phox-/-}$ mice at 24 h after i.c.v. A$\beta_{1–42}$. Mean ± SEM ($n = 6$), *$p < 0.05$

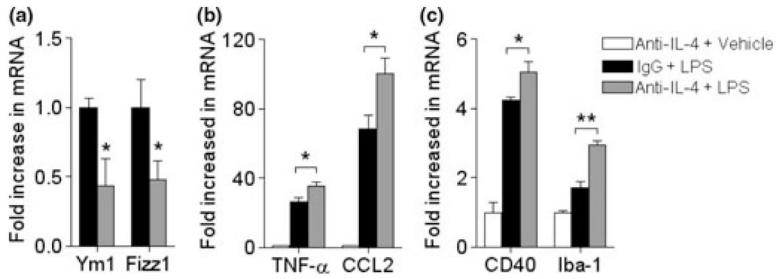

Fig. 7.

Effects of IL-4 neutralization on LPS-induced microglial activation. (a–c) Quantitative real-time PCR analysis showing expression of Ym1, Fizz1, TNF-α, CCL2, CD40, and Iba-1 mRNA (relative to Pgk1) in IgG-treated or IL-4 neutralizing antibody-treated $p47^{phox-/-}$ mice. RNA samples were prepared from brains of WT and $p47^{phox-/-}$ mice at 24 h after coinjection of LPS and neutralizing antibody. Mean ± SEM ($n = 6$), *$p < 0.05$, **$p < 0.01$.

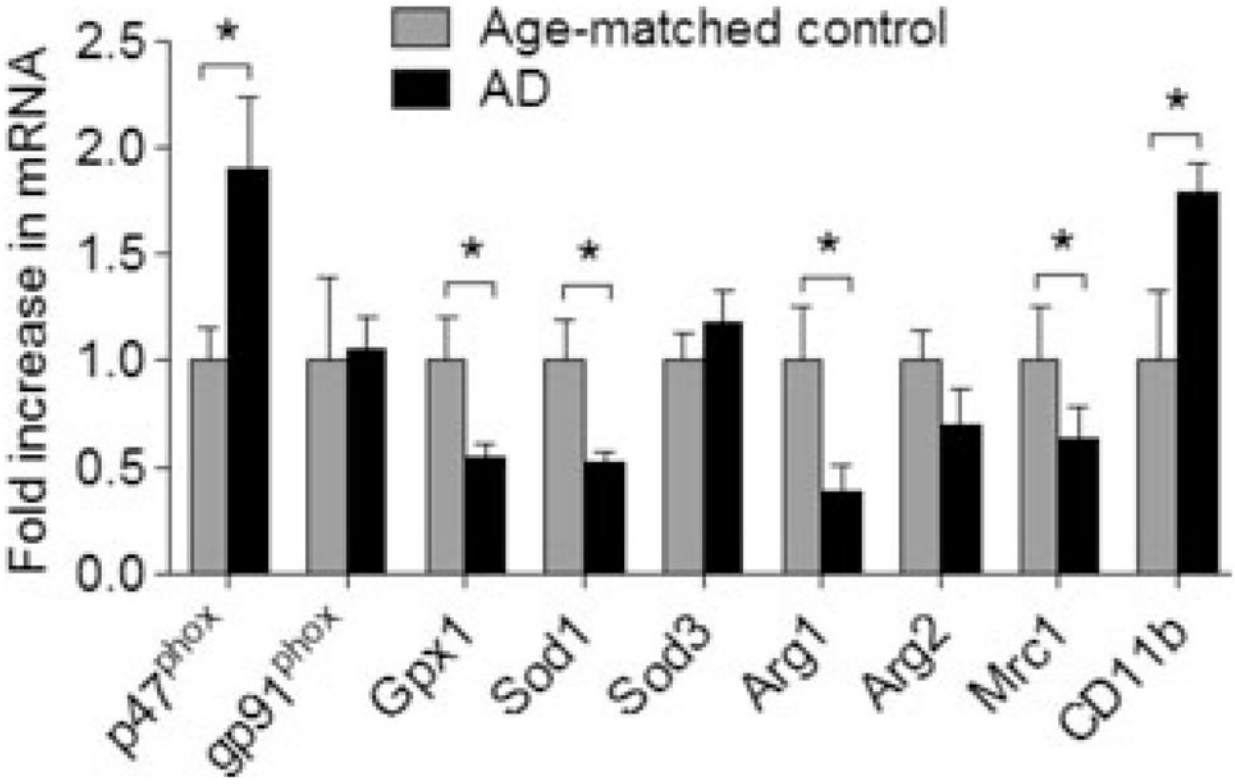

Fig. 8.

Increased p47^{phox} levels in the brain of AD patients. Quantitative PCR showing expression of p47^{phox} and gp91^{phox}, Gpx1, Sod1, and Arg1, Arg2, Mrc1, and CD11b mRNA in AD and age-matched controls by quantitative PCR. Mean ± SEM ($n = 10$), *$p < 0.05$.